

THE DISCOVERY OF A FAINT GLOW OF SCATTERED SUNLIGHT FROM THE DUST TRAIL OF THE LEONID PARENT COMET 55P/TEMPEL-TUTTLE

R. NAKAMURA,¹ Y. FUJII,² M. ISHIGURO,² K. MORISHIGE,³ S. YOKOGAWA,³ P. JENNISKENS,⁴ AND T. MUKAI²

Received 2000 February 8; accepted 2000 May 1

ABSTRACT

A meteoric cloud is the faint glow of sunlight scattered by small meteoroids in the dust trail along the orbit of a comet as seen by an earthbound observer. While these clouds were previously only known from anecdotes of past meteor storms, we now report the detection of a meteoric cloud by modern techniques in the direction of the dust trail of comet 55P/Tempel-Tuttle, the parent of the Leonid meteor stream. Our photometric observations, performed on Mauna Kea, Hawaii, reveal the cloud as a local enhancement in sky brightness during the Leonid shower in 1998. The radius of the trail, deduced from the spatial extent of the cloud, is approximately 0.01 AU and is consistent with the spatial extent mapped out by historic accounts of meteor storms. The brightness of the cloud is approximately $\sim 2\%$ – 3% of the background zodiacal light and cannot be explained by simple model calculations based on the zenith hourly rate and population index of the meteor stream in 1998. If the typical size of cloud particles is $10\ \mu\text{m}$ and the albedo is 0.1, the brightness translates into a number density of $1.2 \times 10^{-10}\ \text{m}^{-3}$. The meteoroid cloud would be the product of the whole dust trail and not only the part that was crossed in 1998.

Subject headings: comets: individual (55P/Tempel-Tuttle) — dust, extinction — interplanetary medium — meteors, meteoroids

1. INTRODUCTION

A cometary dust tail consists of small submicron-sized dust particles that are blown out by solar radiation pressure forces. Larger dust particles form the dust coma and later spread in the orbit of the comet as a result of small differences in orbital period. They form a tubular structure around the parent comet's orbit called a dust trail. Dust trails have been discovered by the *Infrared Astronomical Satellite* (Sykes & Walker 1992). If the Earth comes close enough to the comet's orbit, the entry of such particles into the atmosphere can be observed as meteors, and such dust particles are called meteoroids. Annual streams are caused by particles that have been dispersed from the initial dust trail. We expect outburst activity of a meteor stream if the Earth crosses the dust trails itself, with the highest rates just after the return of the parent comet.

Meteor storms are an impact hazard for satellites. Accurate models are needed to predict such events correctly. Unfortunately, the formation processes of such trails are not well understood because the models include many unknown parameters, such as the comet's past activity, the size-dependent ejection velocities (Whipple 1951; Nakamura & Hidaka 1998), and the effect of gravitational perturbations by the planets and solar radiation pressure forces on the dust's orbital evolution (Brown & Jones 1998). Moreover, little is known about the content of the small grains that are too small to cause visible meteors but typically cause the highest impact hazard because of their abundance.

If we observe the dust trail from the inside, sunlight scattered by the meteoroids should yield a dim glow in the sky called the meteoric cloud. There is anecdotal evidence that such a glow was seen by visual observers during the 1833 storm, but there has been no convincing detection until now (Richter, Leinert, & Planck 1982). A modern cooled CCD camera with a wide-angle lens has the potential to detect such faint and diffuse structures, as demonstrated by the recent identification of asteroidal dust bands (Ishiguro et al. 1999). The best chance to observe the meteoroid cloud is during a significant meteor shower, when the spatial density of meteoroids is high and the line of sight in the tangential direction of the trail is long.

The Leonid shower is famous because of its spectacular historic outbursts (Kresak 1993; Jenniskens 1995) and is our best chance to predict the presence of large dust densities. Historical records imply that an outburst occurs when the distance between the Earth and the descending node of the parent comet P/Tempel-Tuttle is smaller than 0.01 AU and the Earth crosses the cometary orbital plane after the perihelion passage (Yeomans 1981). These conditions were fully met in 1998, and we actually observed a meteor shower with a maximum zenith hourly rate (ZHR) of more than 300 (Jenniskens 1999). Figure 1 shows the appearance of a model trail along the orbit of P/Tempel-Tuttle when the Earth is located in the middle of the trail. We assume that the cross section of the trail is a circle with a 0.01 AU radius. Because of the almost retrograde orbit of P/Tempel-Tuttle, the model cloud is observed in a direction close to the radiant of the shower and extends approximately 4° on the sky for lines of sight longer than 0.3 AU. Our observations and data analyses are described in § 2, and the results are presented in § 3. We discuss the implications of the discovery of the meteoric cloud in § 4.

2. OBSERVATIONS AND DATA ANALYSIS

We made photometric observations of this region of the sky between 1:35 and 5:05 HST on 1998 November 17,

¹ Information Processing Center, Kobe University, Kobe 657-8501, Japan.

² Graduate School of Science and Technology, Kobe University, Kobe 657-8501, Japan.

³ Graduate School of Science, University of Tokyo, Tokyo 113-8654, Japan.

⁴ SETI Institute, NASA Ames Research Center, Mail Stop 239-4, Moffett Field, CA 94035-1000.

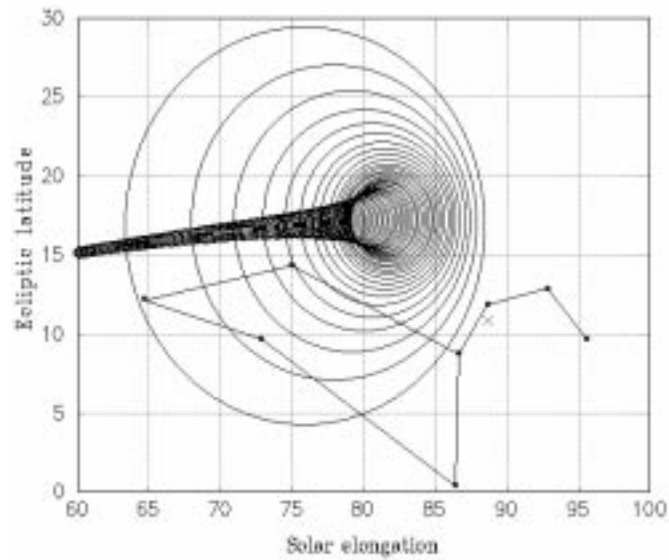


FIG. 1.—Model dust trail seen on 1998 November 17 with the constellation Leo. The horizontal and vertical axes denote the solar elongation angle and the ecliptic latitude, respectively. The trail is assumed to be a cylindrical tube with a radius of 0.01 AU along the orbit of comet P/Tempel-Tuttle. The cross denotes the location of the radiant.

using a wide-angle lens (Sigma 24 mm lens, $F = 2.8$) attached to a cooled CCD camera (Mutoh CV-16), from a location atop Mauna Kea, Hawaii, at an altitude of 4200 m. The angular resolution and the field of view are 2.50 pixel^{-1}

and $32^\circ \times 21^\circ$, respectively. The transmittance spectrum of the filter used is designed to agree with the broadest window of visible airglow and artificial sky lines between Hg at 435 nm and OH at 557.7 nm. The exposure time was set to 3

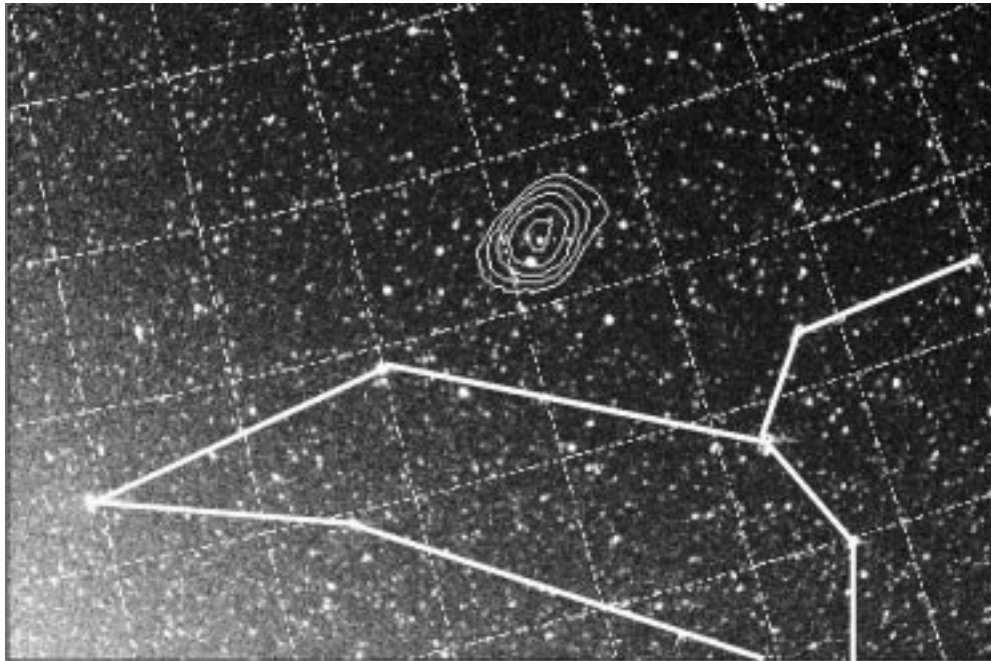


FIG. 2.—Sky image taken at 15:04 UT on November 17 atop Mauna Kea, Hawaii. Contributions from integrated starlight and scattering by the lower atmosphere have been removed from the sky brightness, but the stars remain, and the grid lines are drawn with the same intervals as in Fig. 1 for comparison. The sky brightness, dominated by zodiacal light, increases toward the lower left corner as the solar elongation and ecliptic latitude decrease. After subtraction of the airglow continuum and zodiacal light, the residual component is superimposed as a contour map with increments of $0.5 S_{10\odot}$. A meteoric cloud was found at the expected location (see Fig. 1) with a peak intensity of $4.5 S_{10\odot}$, while the brightnesses of the zodiacal light amount to $200 S_{10\odot}$ at the center of the image.

minutes, and the temperature of the CCD chip was kept at -30° C. In order to check the dark and readout noise during these observations, 49 dark frames were obtained throughout the night. The calibration frames for flat-fielding were taken by the same instrument inside the integrating sphere in the National Institute of Polar Research (NIPR), Tokyo, Japan. Our best result was the last frame, taken just before dawn, because it had the smallest zenith angle. We will consider this frame for further analysis. The remaining frames allow us to estimate the optical depth $\tau(z)$ of atmospheric extinction through photometry of standard stars from the changing zenith angles. From photometry of solar analog stars, it has been found that 1 analog-to-digital converter unit (ADU) on our system is equal to $3.41 S_{10\odot}$ ($= 1.28 \times 10^{-8} \text{ W m}^{-2} \text{ sr}^{-1} \mu\text{m}^{-1}$ at 500 nm).

After removing the stars, we applied a Savitzky-Golay smoothing filter (Press et al. 1988) to obtain the sky brightness. On a moonless night, observed sky brightness (I_{obs}) consists of light from several different sources, i.e., zodiacal light (I_{ZL}) including the contribution from the meteoric cloud, airglow from the upper atmosphere (I_{AG}), integrated starlight of unresolved stars (I_{ISL}), and light scattered by the Earth's atmosphere (I_{sca}). That is,

$$I_{\text{obs}} = (I_{\text{ZL}} + I_{\text{AG}} + I_{\text{ISL}}) \times \exp(-\tau_{\text{eff}}(z)) + I_{\text{sca}}, \quad (1)$$

where $\tau_{\text{eff}}(z)$ denotes the effective optical depth for the extinction of diffuse light sources at zenith distance z . We estimate $\tau_{\text{eff}}(z)$ by using the empirical formula $\tau_{\text{eff}}(z) \simeq 0.75\tau(z)$ (Hong et al. 1998). I_{ISL} is calculated by interpolating Pioneer's data cited in Leinert et al. (1998), and I_{sca} comes from the formulae by Dumont (1965).

The resulting image, after these reduction procedures, is shown in Figure 2. The zenith angle dependence of I_{AG} is described by the van Rhijn function (van Rhijn 1919), but normalization must be done at the zenith. Furthermore, we must subtract the smooth component of the zodiacal light I_{ZL} to extract the faint meteoric cloud. We have constructed a model of zodiacal light in which the spatial distribution function of interplanetary dust particles and the scattering function were taken from Kelsall et al. (1998) and Hong (1985), respectively. The tilt of the symmetry plane of the zodiacal light and I_{AG} at the zenith were determined simul-

taneously by a simplex method, so that the combination gave an optimal fit to the off-cloud regions in the observed data. The regions with large zenith angles were excluded from this fitting procedure in advance.

3. RESULTS

We subtracted I_{AG} and I_{ZL} from the background image and superimposed the resulting structure as the contours in Figure 2. The peak intensity of the meteoric cloud is approximately $4.5 S_{10\odot}$, while I_{ZL} amounts to approximately $200 S_{10\odot}$ at the center of the frame, and I_{AG} at the zenith is $90 S_{10\odot}$. The interval between the contour lines is $0.5 S_{10\odot}$, and the fluctuation of sky brightness, caused mainly by photon noise and dark current, is approximately $1 S_{10\odot}$. Although the shape is rather elongated in the orbital plane of P/Tempel-Tuttle, possibly because of anisotropy in the ejection velocities, the location and extent of the meteoric cloud are consistent with the prediction shown in Figure 1. If a star is bright enough to have a blooming tail, it produces a halo, as shown in Figure 3. The region around the contour map, however, is free from halos because stars of similar magnitude to those in the contour map show no indication of halos. The recently discovered lunar sodium tail induced by the meteor shower (Smith et al. 1999) cannot be responsible for this structure since our filter cuts out the neutral sodium emission at 589.1 nm, as noted before. In order to further check the possibility that the diffuse structure resulted from unknown diffuse sources, either beyond the solar system or within the Earth's atmosphere, on 1998 December 20 we performed the same observations as in November and applied the same reduction procedures. As the diffuse structure found on November 17 was not detected (Fig. 3), the connection with the Leonid meteor activities was established.

Wu & Williams (1996) have shown that the outburst activities of the Leonid meteor stream are caused by relatively young dust particles that have completed only a few orbits since ejection from the nucleus. On the other hand, small and young meteoroids cannot contribute to the cloud because of radiation pressure forces, as shown below. For simplicity, we consider the meteoroids released at perihelion and neglect the effect of ejection velocity. Then a meteor-

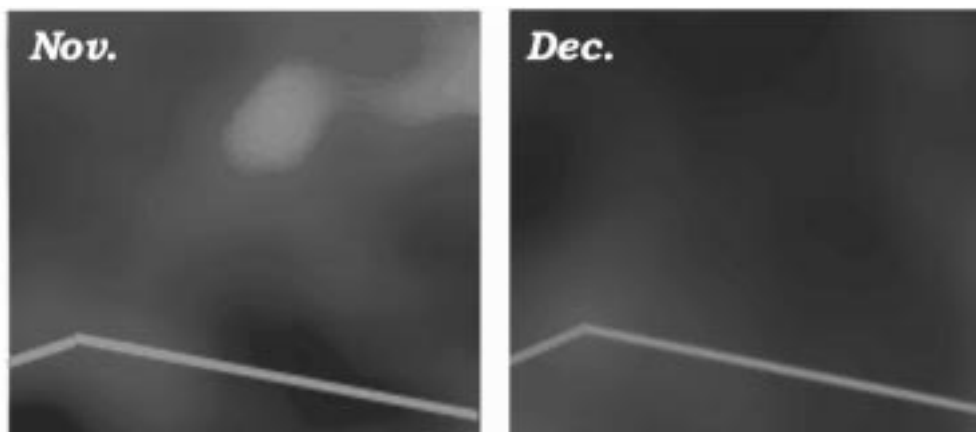


FIG. 3.—Left: Sky on November 17, indicating the presence of the meteoric cloud. A second bright spot is the halo yielded by the bright star Zosca of Leo. Right: Same field as the left panel taken on December 20.

oid's eccentricity and perihelion distance are given by

$$e = (1 - \beta)^{-1}(e_p + \beta), \quad (2)$$

$$q = q_p(1 + e_p)(1 + e)^{-1}(1 - \beta)^{-1}, \quad (3)$$

where β represents the ratio of the radiation pressure force to the gravitational force acting on the meteoroid and q_p and e_p denote the perihelion distance and the eccentricity of the parent comets, respectively (Kresakova 1974; Mukai 1985). Using these equations, we calculated the meteoroids' orbital periods and found that meteoroids with β larger than 0.001 cannot return to the vicinity of the Earth's orbit along with P/Tempel-Tuttle. If the meteoroids consist of astronomical silicate, $\beta = 0.001$ corresponds to a radius of roughly $100 \mu\text{m}$. Assuming a simple power-law size distribution of meteoroids with this lower limit, we can estimate the brightness of the meteoric cloud as follows. The mass M and magnitude m of a meteoroid are assumed to obey a simple power law as $M(m) = M(0) \times 10^{-\alpha \times m}$, where $M(0)$ is the mass of a zero magnitude meteor. On the other hand, the meteor flux $n(m)$ and the population index χ are determined as $n(m) = n(0) \times \chi^m$ by visual observations. The expressions of $n(0)$ and $M(0)$ for Leonid can be found in Jenniskens (1994). The two equations give the mass distribution function of the meteoroids as

$$n(M) = \kappa \times M^\gamma, \quad (4)$$

where

$$\begin{aligned} \kappa &= -\ln 10 \times \alpha \times n(0) \times M(0)^{\log \chi/\alpha}, \\ \gamma &= -(1 + \log \chi/\alpha). \end{aligned} \quad (5)$$

If this power law covers the whole size range, we can obtain the total scattering cross section by size integration. As long as $\gamma \leq 5/3$, the total scattering cross section is dominated by the lower limit of meteoroid size and is insensitive to the upper limit. The upper limit is set to 10 cm throughout this paper. When meteoroids are distributed uniformly in the trail, the mean volume scattering function of the meteoroids inside the trail is given simply by dividing the total cross section by the relative velocity of the Leonid meteors and the Earth. The brightness of the scattered sunlight is the product of this mean volume scattering function,

the solar flux, the length of the line of sight L , and the albedo A of the meteoroids (Richter et al. 1982).

Figure 4 shows the brightness as a function of α and χ for a maximum ZHR = 300, as observed in the Leonid outburst in 1998. The meteoric cloud is assumed to be a direct result of an outburst of meteor stream activities associated with the return of P/Tempel-Tuttle. Based on the dynamical restrictions discussed above, we estimate the lower limit in the size integration to be $100 \mu\text{m}$. It follows from Figure 4 that the observed cloud brightness cannot be explained by a simple power-law size distribution unless $\alpha \sim 0.4$ and $\chi \geq 3.5$. In high-velocity streams such as Leonid, the luminosity I of a meteor could be proportional to the kinetic energy (Jacchica, Verniani, & Briggs 1967). In this case, $I \sim M \sim 10^{-0.4 \times m}$ and consequently α equals 0.4. However, visual observations of the Leonid meteor stream in 1998 reported much lower values for χ . Furthermore, numerous meteoroids around $400 \mu\text{m}$ in size should have been detected as faint meteors by the video imaging instruments on board the *Leonid MAC* mission (Jenniskens & Butow 1999). Therefore, the size distribution and/or spatial density of meteoroids in the local volume swept by the Earth must be significantly different from the global average, provided that the meteoric cloud is directly related to the outburst of meteor stream activities.

4. DISCUSSION

The observed flux $2S_{1,0\odot}$ at the outermost lines in Figure 2 corresponds to a total scattering cross section density of $3.7 \times 10^{-20} \text{ m}^2 \text{ m}^{-3}$. If the meteoroids consist of spherical particles $100 \mu\text{m}$ in size, a spatial number density of $1.2 \times 10^{-12} \text{ m}^{-3}$ leads to a huge discrepancy with the results from video imaging of faint meteors, as noted before. On the other hand, the critical value for bound orbits is derived as $\beta_c = (1 - e_p)/2$ from equation (2). Substituting $e_p = 0.906$ for P/Tempel-Tuttle, we obtain $\beta_c = 0.047$, which corresponds to approximately $4 \mu\text{m}$ meteoroids consisting of astronomical silicate. Thus, the typical size of meteoroids responsible for the cloud would be several tens of microns. If the typical size is $10 \mu\text{m}$ and the albedo is 0.1, the number density is approximately $1.2 \times 10^{-10} \text{ m}^{-3}$. Such meteoroids tend to accumulate at perihelion, as dis-

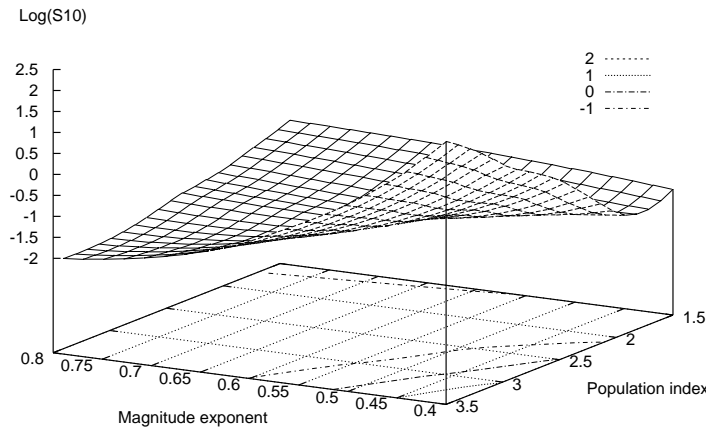


FIG. 4.—Expected cloud brightness in $\log(S_{1,0\odot})$ for zenith hourly rate ZHR = 300, albedo $A = 0.1$, and length of line of sight $L = 0.3 \text{ AU}$. Note that the brightness is proportional to ZHR, A , and L . The horizontal axis denotes the exponent in the mass-magnitude relation, and the vertical axis is the population index deduced from visual observations of meteors. The size distribution of meteoroids is assumed to follow eq. (4) in the text.

persion is negligible according to equation (3), despite the significant increase in their orbital period. Such small meteoroids can be included in the diffuse and spatially uniform trail, which causes the annual activities of the meteor stream, and contribute to the observed brightness of the cloud. In this case, we should be able to observe the Leonid cloud irrespective of the occurrence of outburst. Also, it is likely that meteoric clouds are also associated with other major meteor streams, such as the Perseid, Quadrantids, Orionids, and Draconid, whose parent comets are currently far from perihelion.

This work is supported by a grant from the US Air Force Office of Scientific Research. The 1998 *Leonid MAC* was sponsored by NASA's Planetary Astronomy and Exobiology Programs, the NASA/Ames Research Center, and the NASA/ARC Advanced Missions and Technologies Program for Astrobiology. We thank the members of the SUBARU Project office in Hilo, Hawaii, for providing us with the opportunity to make observations on Mauna Kea. We also thank Makoto Taguchi (NIPR) for his assistance with taking the flat frames at NIPR.

REFERENCES

- Brown, P., & Jones, J. 1998, *Icarus*, 133, 36
 Dumont, R. 1965, *Ann. d'Astrophys.*, 28, 265 (NASA Tech. Trans. TT-FII, 164)
 Hong, S. S. 1985, *A&A*, 146, 67
 Hong, S. S., Kwon, S. M., Park, Y.-S., & Park, C. 1998, *Earth, Planets and Space*, 50, 487
 Ishiguro, M., Nakamura, R., Fujii, Y., Morishige, K., Yano, H., Yasuda, H., Yokogawa, S., & Mukai, T. 1999, *ApJ*, 511, 432
 Jacchia, L. G., Verniani, F., & Briggs, R. E. 1967, *Smithsonian Contrib. Astrophys.*, 10, 1
 Jenniskens, P. 1994, *A&A*, 287, 990
 ———. 1995, *A&A*, 295, 206
 Jenniskens, P. 1999, *Meteoritics Planet. Sci.*, 34, 959
 Jenniskens, P., & Butow, S. J. 1999, *Meteoritics Planet. Sci.*, 34, 933
 Kelsall, T., et al. 1998, *ApJ*, 508, 44
 Kresak, L. 1993, *A&A*, 279, 646
 Kresakova, M. 1974, *Bull. Astron. Inst. Czechoslovakia*, 25, 191
 Leinert, Ch., et al. 1998, *A&AS*, 127, 1
 Mukai, T. 1985, *A&A*, 153, 213
 Nakamura, R., & Hidaka, Y. 1998, *A&A*, 340, 329
 Press, W. H., et al. 1988, *Numerical Recipes in C* (2d ed.; Cambridge: Cambridge Univ. Press)
 Richter, I., Leinert, C., & Planck, B. 1982, *A&A*, 110, 115
 Smith, S. M., Wilson, J. K., Baumgardner, J., & Mendillo, M. 1999, *Geophys. Res. Lett.*, 26, 1649
 Sykes, M. V., & Walker, R. G. 1992, *Icarus*, 95, 180
 Van Rhijn, P. J. 1919, *ApJ*, 50, 356
 Whipple, F. L. 1951, *ApJ*, 113, 464
 Wu, Z., & Williams, I. P. 1996, *MNRAS*, 280, 1210
 Yeomans, D. K. 1981, *Icarus*, 47, 492